MIT Joint Program on the Science and Policy of Global Change

Transient climate change and potential croplands of the world in the 21st Century*

X. Xiao, C. Vörösmarty, J.M. Melillo, D.W. Kicklighter, H. Tian, A.D. McGuire, Y. Pan, and Z. Yang

Reprint Series Number JP 99-015

** Reprinted with permission from Telespazio S.p.A. From Sistema Terra 8(1–3):96–109, December 1999.*

The MIT Joint Program on the Science and Policy of Global Change is an organization for research, independent policy analysis, and public education in global environmental change. It seeks to provide leadership in understanding scientific, economic, and ecological aspects of this difficult issue, and combining them into policy assessments that serve the needs of ongoing national and international discussions. To this end, the Program brings together an interdisciplinary group from two established research centers at MIT: the Center for Global Change Science (CGCS) and the Center for Energy and Environmental Policy Research (CEEPR). These two centers bridge many key areas of the needed intellectual work, and additional essential areas are covered by other MIT departments, by collaboration with the Ecosystems Center of the Marine Biological Laboratory (MBL) at Woods Hole, and by short- and long-term visitors to the Program. The Program involves sponsorship and active participation by industry, government, and non-profit organizations.

To inform processes of policy development and implementation, climate change research needs to focus on improving the prediction of those variables that are most relevant to economic, social, and environmental effects. In turn, the greenhouse gas and atmospheric aerosol assumptions underlying climate analysis need to be related to the economic, technological, and political forces that drive emissions, and to the results of international agreements and mitigation. Further, assessments of possible societal and ecosystem impacts, and analysis of mitigation strategies, need to be based on realistic evaluation of the uncertainties of climate science.

This report is one of a series intended to communicate research results and improve public understanding of climate issues, thereby contributing to informed debate about the climate issue, the uncertainties, and the economic and social implications of policy alternatives.

Henry D. Jacoby and Ronald G. Prinn,
Program Co-Directors

For more information, contact the Program office:

MIT Joint Program on the Science and Policy of Global Change
Postal Address:
77 Massachusetts Avenue
MIT E40-271
Cambridge, MA 02139-4307 (USA)
Location:
One Amherst Street, Cambridge
Building E40, Room 271
Massachusetts Institute of Technology
Access:
Tel: (617) 253-7492
Fax: (617) 253-9845
E-mail: ***globalchange@mit.edu***
Web site: ***http://web.mit.edu/globalchange/www/***

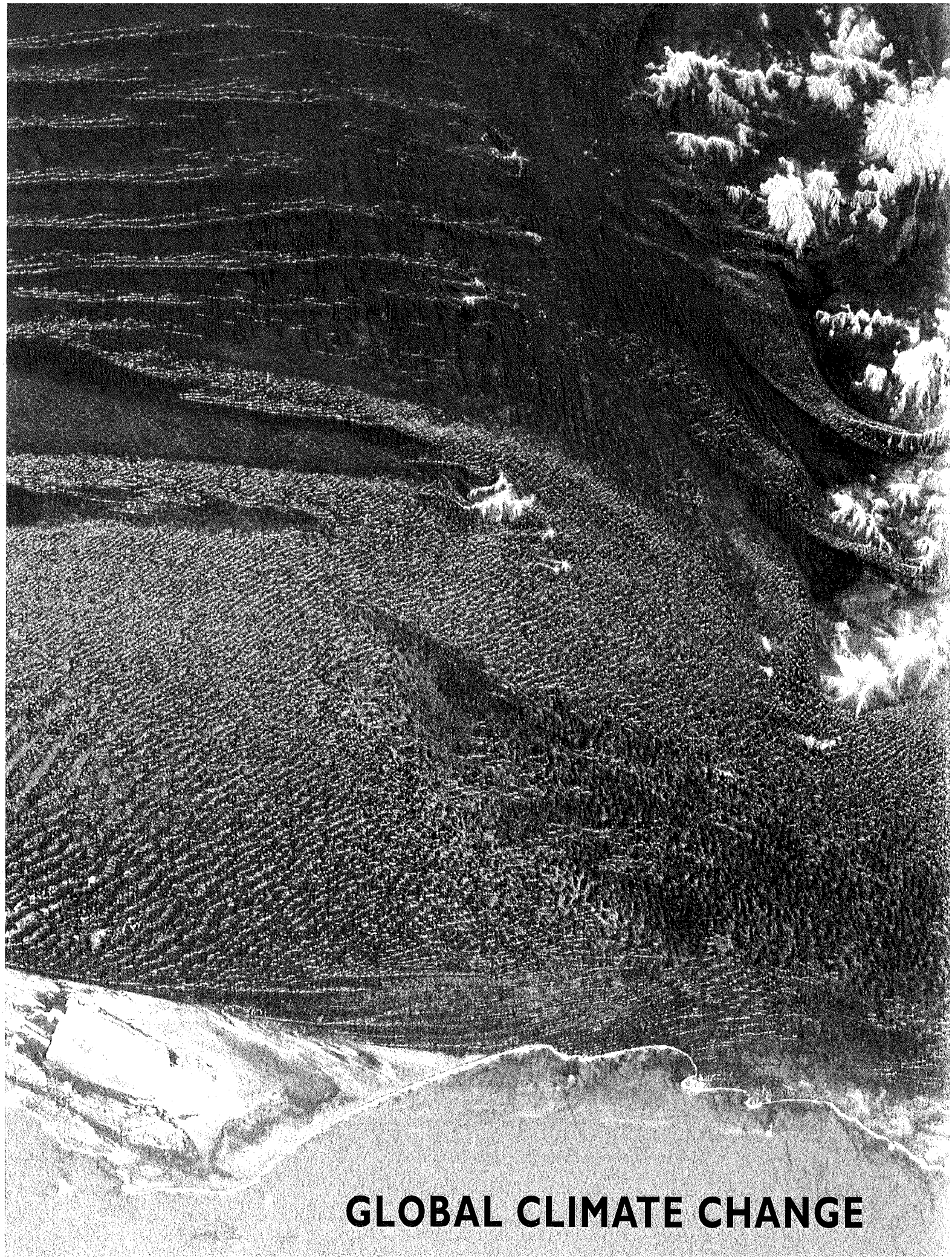
GLOBAL CLIMATE CHANGE

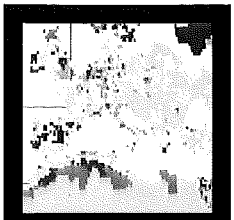

Keywords
Agriculture, Croplands, Climate Change, Model, Globe

In this paper we develop a cropland distribution model that includes constraints of climate, soil and topography on spatial distribution of potential croplands globally. The model was applied to estimate the area and spatial distribution of global potential croplands on the basis of contemporary climate and to assess the sensitivity of potential croplands to the three transient climate change predictions in the 21st century as projected by the Integrated Global System Model. The model estimates an area of about 32.79 10^6 km^2≤ global potential croplands under contemporary climate conditions. Global potential croplands

Transient climate change and potential croplands of the world in the 21st century

Xiangming Xiao, Charles J. Vörösmarty, Complex System Research Center, Institute for the Study of Earth, Oceans and Space, University of New Hampshire, Durham
Jeyy M. Melillo, David W. Kicklighter, Hanqin Tian, The Ecosystems Center, Marine Biological Laboratory, Woods Hole
A. David McGuire, Institute of Artic Biology, University of Alaska, Fairbanks, USA
Yude Pan, Forest Service, US Department of Agricolture, Randor, PA 19087, USA
Zili Yang, The Joint Program on the Science and Policy of Global Change, Massachusetts Institute of Technology, Cambridge, USA

Introduction

Human population of the world is increasing by about 1.5% per year and is projected to double by the end of 21st century. Increasing human population and higher demand for food may require both expansion of land used for crop production and higher yield per unit area of croplands to provide enough food supplies for people. It has been estimated that deforestation and land conversion to agriculture was about 0.3 hectare for each additional person in 1700-1980 for the whole world, and 0.2 hectare per additional person in 1950-1980 for the developing countries (Grübler 1994). Using 0.2 hectare per person, Grübler (1994) estimated that an increase of 10 of 10^6 km^2 arable lands would be needed for additional 5 billion world population in the 21st century. Agricultural production per unit area has increased substantially over the last few decades due to irrigation, fertilization, mechanization and new crops of higher yield and stronger resistance to pest and disease. Intensive agricultural production, however, is under increasing constraints of energy and resources, e.g., fertilizer, water and soils (Naylor 1996). Land degradation and desertification are reducing the areas of fertile lands for agriculture production (Bullock and Le Houerou 1996). At present, soil erosion has resulted in a loss of croplands of about 0.06 to 0.07 10^6 km^2 per year, and soil salinization has already affected up to 8% (0.2 10^6 km^2) of the 2.53 10^6 km^2 currently irrigated croplands (World Resource Institute 1992). Rapid expansion of urbanization has also resulted in significant losses of agricultural lands, especially in developing countries. Cultivable land per capita in China has declined by approximately 20% since 1978, mostly due to rural industrialization and small-town growth (Bradbury *et al.* 1996). Urban areas currently account for about 1% of the global land area and may increase to occupy 2% of the global land area by 2100 (Douglas 1994). Therefore, future trends in the area and spatial distribution of land suitable for crop production are likely to have significant impacts on sustainable agriculture and environment in the 21st century.

The United Nations Food and Agriculture Organization (FAO) has developed the agro-ecological zone approach to assess land suitability for croplands at local and national scales, which is based on climate, soil and crop characteristics (FAO 1978, Brinkman 1987, FAO/IIASA 1993). Earlier studies (Leemans and Solomon 1993, Cramer and Solomon 1993) have applied climate-based models to estimate the area and spatial distribution of croplands over the globe. Cramer and Solomon (1993) modeled the global distribution of potential croplands under the contemporary climate and under doubled CO_2 equilibrium climates generated by four atmospheric general circulation models. Their results indicated that climate change significantly affects the area and spatial distribution of land that can potentially be used for crop production. However, topographical constraint on cropland distribution was not explicitly included in the above global-scale studies, and consequently the area of potential croplands is likely to be substantially overestimated.

To better evaluate suitability and availability of land potential for agriculture is an essential part of the efforts in modeling and planning of land use and land cover change. The objectives of this study are twofold: (1) to improve the estimates of area and spatial distribution of potential croplands in the world under the contemporary climate, and (2) to quantify the impacts of transient climate change in the 21st century on the area and spatial distribution of potential croplands in the world. In this study we develop a cropland distribution model that includes climate, soil and topography constraints on the spatial distribution of potential croplands. We first applied the model to estimate the area and spatial distribution of potential croplands of the world under the contemporary climate. Secondly, we applied the model to assess the effect of transient climate change on potential croplands, using three transient climate change predictions over the period of 1977-2100 from the Integrated Global System Model (IGSM, Prinn *et al.* 1999, Xiao *et al.* 1998) for assessment of climate change. We examined the spatial patterns and temporal dynamics of potential croplands at the

scales of the globe, economic regions and grid cells.

Description of the cropland distribution model

Climate constraints

Heat and water requirements of crops determine the spatial distribution of potential croplands. In a correlation analysis between the map of croplands (Olson *et al.* 1983) and maps of climate variables generated from the IIASA database of contemporary climate (Leemans and Cramer 1991), Cramer and Solomon (1993) defined a climate envelope of potential croplands: equal or greater than 2000 growing degree days (GDD, 0 °C base), a ratio of actual evapotranspiration over potential evapotranspiration (AET/PET) greater than 0.45; excluding those areas that have a temperature of greater than 15.5 °C in the coldest month and a AET/PET ratio of greater than 0.70, where potential severe soil erosion in croplands would limit crop production.

In this study we use the above climate envelope (Cramer and Solomon, 1993) to define climate-based potential croplands, although our procedures to calculate AET/PET ratios is slightly different from Cramer and Solomon (1993). In our study, monthly mean temperature data are linearly interpolated to daily mean temperature, which are then used for calculating growing degree-days (GDD). We use the water balance model of Vörösmarty *et al.* (1989) to estimate monthly PET and AET. The water balance model has been incorporated into our Terrestrial Ecosystem Model (TEM, Raich *et al.* 1991, Melillo *et al.* 1993, McGuire *et al.* 1997, Xiao *et al.* 1997, 1998, Prinn *et al.* 1998) and runs with a monthly time step. The input variables of the water balance model include elevation, soil texture (proportion of sand, clay and silt), monthly climate (temperature, precipitation and cloudiness) and vegetation types. Elevation is used to determine snowmelt dynamics of a grid cell (snowmelt occurs in one month if elevation is below 500 m; snowmelt occurs in two months if elevation is above 500 m). Soil texture affects the field water-holding capacity and wilting point of soils. The monthly flux PET is calculated as a function of monthly mean air temperature and solar radiation (Jensen and Haise 1963). The flux of AET is equal to PET in wet months but is modeled as a function of rainfall, snowmelt recharge and a change of soil moisture in dry months (Vörösmarty *et al.* 1989). The ratio of AET/PET for each of 12 months is calculated. For moist tropical regions where temperature in the coldest month is greater than 15.5 °C, we assume that a grid cell will not be suitable for croplands if there are more than eight months in a year that have a AET/PET ratio > 0.70.

Topographical constraints

Cropland distribution is also constrained by topographical features such as slope and aspect, because cropland is vulnerable to soil erosion and there is low stability of slope in mountainous regions. In land use planning at the fine spatial scale, slope and aspect are widely used to determine whether land is suitable for crop cultivation. However, at large spatial scales such as 0.5 latitude 0.5 longitude (approximately 55 km in equator), actual slopes generally cannot be derived. Instead, we use elevation data directly to define mountains. Mountain systems account for roughly 20% of the global land area (Beniston and Fox 1996). Mountain regions are characterized by multiple land uses, e.g., forestry, minerals mining, hydropower plants and tourism.
For defining mountains from elevation data, we designed a pattern search algorithm within a window of 3x3 grid cells. We calculate elevation differences between the center grid cell and each of its eight neighboring grid cells. We first recognize or stratify three topographical features of the world: plains with low elevation (less than 500 m in elevation); low mountains and low plateau (less than 1000 m in elevation); high mountains (e.g., Rocky mountains in North America, Andes in South America, Himalaya mountains) and high plateaus (e.g., Qinghai-Tibet plateau in China). Then, we apply the following criteria to decide whether the center grid cell is mountain: (1) elevation difference is greater than 400 m, when elevation of the center grid cell is less than 500 m; (2) elevation difference is greater than 600 m, when elevation of the center grid cell is within 500-1000 m; and (3) elevation difference is greater than 1200 m, when elevation of the center grid cell is more than 1000 m. If any of the eight elevation differences within a 3x3 window meets one of the three criteria, then the center grid cell is assigned to be mountain. If a grid cell is assigned to be mountain, it will not be used for cropland, even if it meets climate constraints for croplands. We applied this 3x3 window pattern search to all the grid cells in a global elevation database (NCAR/NAVY 1984) with a resolution of 0.5 (longitude) 0.5 (latitude) grid. The resulting global map of mountains (fig. 2) clearly shows large mountain ranges, e.g., Rocky mountains, Andes mountains and Qinghai-Tibet plateau. In a visual qualitative comparison, the geographical distribution of mountains in our global map of mountains mimics well with a shaded relief image of global topography (Sloss 1996), which was generated from an elevation data set (NOAA's ETOPO5) with a spatial resolution of 5 minute (latitude) by 5 minute (longitude).

increase in the 21st century and in 2100 reach about +6.9% (2.25 10^6 km^2) for the LLH (lower CO_2 emissions and temperature increases), +11.6% (3.80 10^6 km^2) for the RRR (reference CO_2 emissions and temperature increases), and +12.6% (4.13 10^6 km^2) for the HHL (higher CO_2 emissions and temperature increases) transient climate change predictions. Among 12 economic regions of the world, the Former Soviet Union and the Other OECD Countries regions have the largest increases in potential croplands, while developing countries have little increases in potential croplands. Spatial distribution of potential croplands changes considerably over time, dependent upon the transient climate change predictions

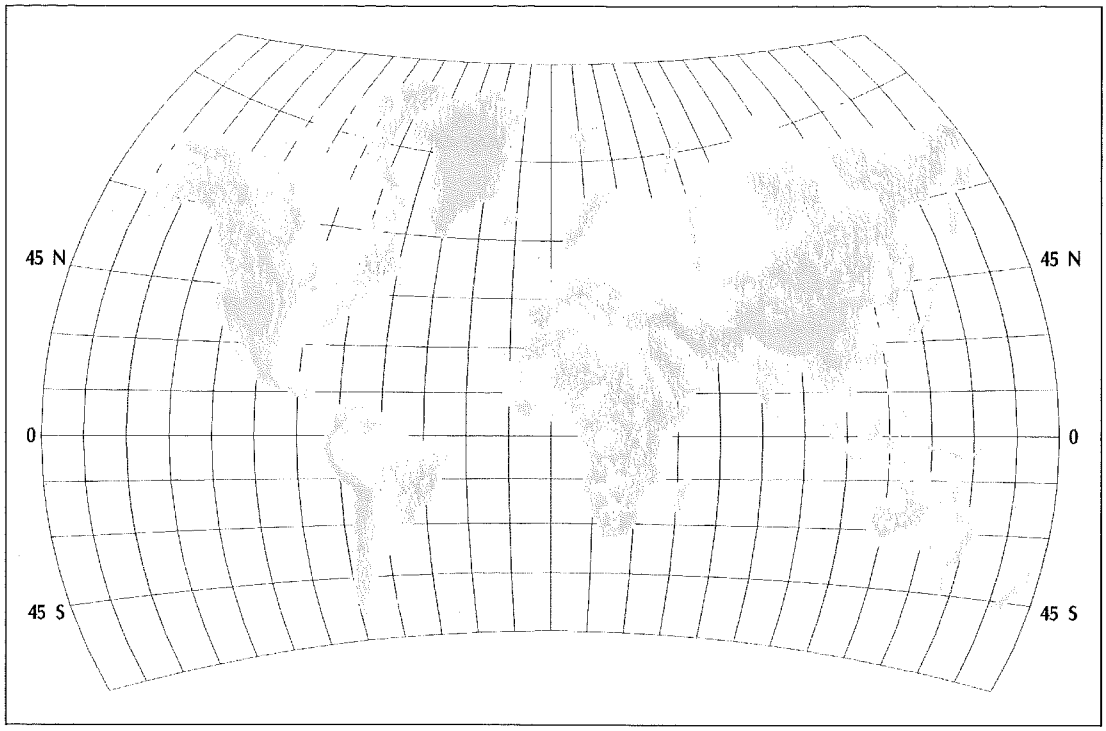

1. *Spatial distribution of mountains in the world, as simulated by the 3x3 window pattern search procedure. Note that Greenland is mostly covered with ice*

Data for a global extrapolation of the cropland distribution model

The application of the cropland distribution model to a grid cell requires data of monthly climate (precipitation, mean temperature and mean percent cloud coverage), soil texture (proportion of sand, silt and clay), elevation and vegetation types. Soil texture and vegetation types are used to define the soil – and vegetation – specific (e.g., rooting depth) parameters for a grid cell. For a global extrapolation of the cropland distribution model, we use the spatial data sets that are organized at a spatial resolution of 0.5 (longitude) 0.5 (latitude). At 0.5 resolution, global land areas are represented by 62,483 grid cells. We use a global potential natural vegetation data set (see Melillo *et al.* 1993), which includes 3059 grid cells of ice and 1525 grid cells of floodplain and wetlands (e.g., mangrove, swamp and salt marsh). Thus, the global land area used in this study is 133.56 10^6 km^2, i.e., 130.31 10^6 km^2 upland and 3.25 10^6 km^2 wetlands. In calculating potential croplands, we exclude those grid cells that are wetland in the vegetation data set (Melillo *et al.* 1993). For long-term average contemporary climate, we use the Cramer and Leemans CLIMATE database (Wolfgang Cramer, personal communication, 1995), which is a major update of the IIASA Climate database (Leemans and Cramer 1991). The elevation data set we used is an aggregation to 0.5 resolution of a global 10-minute resolution data set (National Center for Atmospheric Research (NCAR)/NAVY 1984). We use the soil texture data set that is based on digitization of the soil map of the world from the United Nations Food and Agriculture Organization (FAO) – United Nations Educational, Scientific and Cultural Organization (UNESCO) (1971). Using the above global data sets we ran the cropland distribution model to estimate spatial distribution of potential croplands under the contemporary climate.

Transient climate change scenarios

To assess the sensitivity of potential croplands to future climate change, we used transient climate change predictions over the period of 1977-2100 from a sensitivity study of the Integrated Global System Model (IGSM, Prinn *et al.* 1999, Xiao *et al.* 1998). The IGSM has been recently developed to address major issues in climate change, impact assessment and climate policy (Prinn *et al.* 1999, Xiao *et al.* 1998). As shown in fig. 1, the IGSM currently includes six component models: the Anthropogenic Emission Prediction and Policy Analysis (EPPA) model (Yang *et al.* 1996), an atmospheric chemistry model (Wang *et al.* 1995, 1998), a 2-dimensional land-ocean climate model (Yao and Stone 1987, Stone and Yao 1987, 1990; Sokolov and Stone 1995, 1998), an ocean carbon model (Prinn *et al.* 1999), a terrestrial biogeochemistry model (the Terrestrial Ecosystems Model, Raich *et al.* 1991, Melillo *et al.* 1993, McGuire *et al.* 1997, Xiao *et al.* 1997, 1998) and natural emission models of N_2O and CH_4 from soils (Liu 1996). The EPPA model projects anthropogenic emissions of CO_2 and other greenhouse gases (e.g., N_2O and CH_4) in the 12 economic regions of the world. The coupled atmospheric chemistry/climate model (Wang *et al.* 1998) uses the projected anthropogenic and

natural emissions of greenhouse gases to predict the evolution of concentrations of chemical species in the atmosphere and their radiative forcing on climate systems. The projected transient changes in climate (temperature, precipitation and cloud coverage) are used to drive the Terrestrial Ecosystem Model (Melillo *et al.* 1993) and the natural emission models of N_2O (Liu 1996).

In the sensitivity study (Prinn *et al.* 1999), the standard parameters and assumptions in the EPPA model and the atmospheric chemistry/climate model were first used to generate the reference (RRR) scenario of changes in anthropogenic emissions of greenhouse gases and climate. Anthropogenic emissions of CO_2 projected by the EPPA model in the RRR scenario are similar to the CO_2 emissions of the IS92a scenario of IPCC (IPCC 1994). Then, the EPPA model projected higher and lower emissions of CO_2 and other greenhouse gases by changing the labor productivity growth, the non-price-induced change in energy efficiency (AEEI rate) and the cost of non-carbon backstop technology (e.g., nuclear, solar and hydropower energy). The anthropogenic emissions of CO_2 and other greenhouse gases were then used to drive the combined atmospheric chemistry/2-D land-ocean climate model. In the 2-D land-ocean climate model, parameters for ocean heat diffusion efficiency, aerosol optical depth and model sensitivity to doubled CO_2 were changed to generate different climate change predictions for a given set of emissions of CO_2 and other greenhouse gases. Seven transient climate change predictions over the period of 1977-2100 have been generated in the sensitivity study (Prinn *et al.* 1999). Here, we used three of the seven transient climate change predictions: (1) the RRR scenario; (2) the HHL scenario that has higher CO_2 emissions from the EPPA model and larger changes in temperature from the climate model which uses parameters of higher temperature sensitivity to doubled CO_2 and lower heat diffusion coefficient into the deep ocean; and (3) the LLH scenario that has lower CO_2 emissions from the EPPA model and smaller changes in temperature from the climate model which uses parameters of lower temperature sensitivity to doubled CO_2 and higher heat diffusion coefficient into the deep ocean (fig. 3). Globally, atmospheric CO_2 concentration and climate vary significantly among the three transient climate change predictions over the period of 1977-2100 (fig. 3). Atmospheric CO_2 concentration in 2100 is about 745 ppmv in the RRR, 936 ppmv in the HHL and 592 ppmv in the LLH scenarios. Global annual mean temperature between 1977 and 2100 increases about 2.6 °C for the RRR, 3.3 °C for the HHL and 1.4 °C for the LLH scenarios. Global

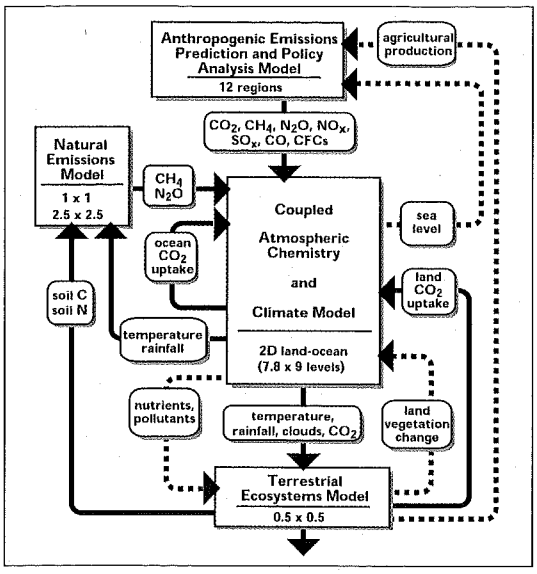

2. *A schematic diagram illustrating the framework and components of the MIT Global System Model for integrated assessment of climate change. The linkages and feedbacks between the component models that are currently included or under development for future inclusion are shown as solid and dashed lines, respectively*

daily precipitation increases slightly over time for the three scenarios. Global mean annual cloudiness decreases in the RRR and the LLH scenarios but increases in the HHL scenario.

The 2-D land-ocean climate model simulates the zonally averaged climate separately over land and ocean as a function of latitude and height. It has 23 latitudinal bands, corresponding to a resolution of 7.826, and nine vertical layers. The climate outputs in the 23 latitudinal bands from the 2-D land-ocean climate model were first linearly interpolated to 0.5 resolution, and the interpolated values were then applied to all the grid cells within a 0.5 latitudinal band. In generating "future climate", we calculated absolute differences in monthly mean temperature and ratios in monthly precipitation and monthly mean cloudiness, using the simulated climate data in 1977 from the 2-D land-ocean climate model as the control values. Then, we added the absolute differences in monthly mean temperature over the period of 1978-2100 to the contemporary monthly mean temperature data, and multiplied the ratios in monthly precipitation and monthly mean cloudiness over the period of 1978-2100 to the contemporary monthly precipitation and monthly mean cloudiness data, respectively.

Results

Potential croplands under contemporary climate

The cropland distribution model estimates that the area of global potential croplands under contemporary climate is about 32.79 10^6 km^2, approximately 25.2% of the global land area (130.31 10^6 km^2). This estimate of global potential croplands is significantly lower than the estimate of 41.53 10^6 km^2 global potential croplands under the contemporary climate data (Leemans and

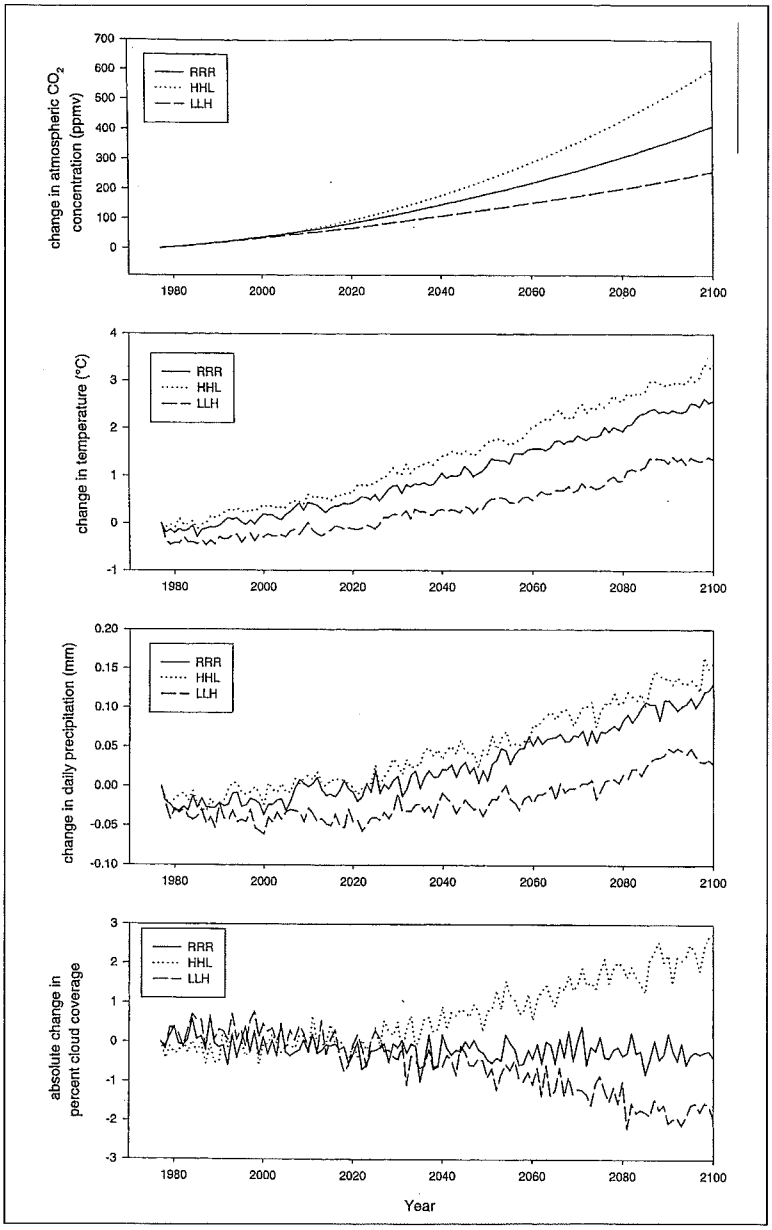

3. *Projected changes in global annual mean atmospheric CO_2 concentration (ppmv), global annual mean temperature (°C), global mean daily precipitation (mm) and global annual mean cloudiness (%) over the period of 1977 - 2100 for the RRR, HHL and LLH predictions by the Integrated Global System Model (see Prinn* et al. *1999)*

Cramer 1991) by Cramer and Solomon (1993). This difference is primarily attributed to the fact that topographical constraint is taken into account in our cropland distribution model. By compiling map data from various data sources, Olson *et al.* (1983) provided a global map of croplands at 0.5 (longitude) 0.5 (latitude) resolution, and Matthews (1983) provided a global map of croplands at 1.0 (longitude) 1.0 (latitude) resolution grid. Our estimate of global potential croplands is about 35.9% higher than the estimate of croplands (about 24.12 10^6 km²) of Olson *et al.* (1983) and is close to the estimate of croplands (about 32.05 10^6 km²) of Matthews (1983).

Potential cropland area varies substantially among the twelve economic regions of the world, as defined in the EPPA model (fig. 4). The ratio of potential cropland area over total land area for each of the economic regions indicates the potential of land for cultivation. The ratio varies from 10.8% in the Energy Exporting Countries (EEX) economic region to 74.3% in the Eastern European Countries (EET) economic region (fig. 4). The EEX and the Rest of the World (ROW) economic regions have large areas of desert and semi-arid land, where there is not enough precipitation to support rain-fed agriculture. The Former Soviet Union (FSU) and the Other OECD Countries (OOE) economic regions have large areas of land in high latitudes where temperature is too low for crops to grow. China has the largest population in the world but a low ratio of potential cropland area over total land area because China has large areas of mountains (fig. 2), dry land (e.g., Mongolia plateau, Gobi desert in northwestern China) and the cold Qinghai-Tibet plateau.

The ratio of actual cropland area over potential cropland area in an economic region indicates the realized potential of land used for cultivation. According to the United Nations Food and Agriculture Organization (FAO) country statistics data of crop cultivation and production (FAO 1980), actual cropland areas among the twelve economic regions in 1980 vary considerably (fig. 4) partly because of the differences in population and agricultural practices. The ratio of actual cropland area over potential cropland area ranges from 25.5% in Brazil to 113.5% in India (fig. 4). Only five economic regions (Brazil, Japan, OOE, FSU, and USA) have a ratio of lower than 50%. The low ratio in Brazil indicates that Brazil has relatively a large amount of potential croplands for future use. The highest ratio in India indicates that people in India have already practiced crop cultivation in mountainous regions and other marginal lands. However, crop cultivation in mountains is generally vulnerable to severe soil erosion and low slope stability in mountains, especially on long-term temporal scales.
As shown in fig. 5, the cropland distribution model represents reasonably well the spatial distribution of global croplands as described in the map of croplands of Olson *et al.* (1983). The agreement between Olson *et al.* (1983) and the cropland distribution model occurs in 6265 grid cells, about 14.35 10^6 km², which accounts for 59.5% of the global cropland area estimated by Olson *et al.* (1983). The disagreement in spatial distribution of croplands occurs largely in semi-arid and arid regions where crop cultivation depends upon irrigation water from rivers or underground water reserves. For example, Olson *et al.* (1983) included irrigated croplands, thus there are fair amounts of croplands along the Nile river and in the semi-arid western US (fig. 5). The cropland distribution model in this study has not included global river networks, thus it fails to project croplands along the Nile river where croplands are completely dependent upon

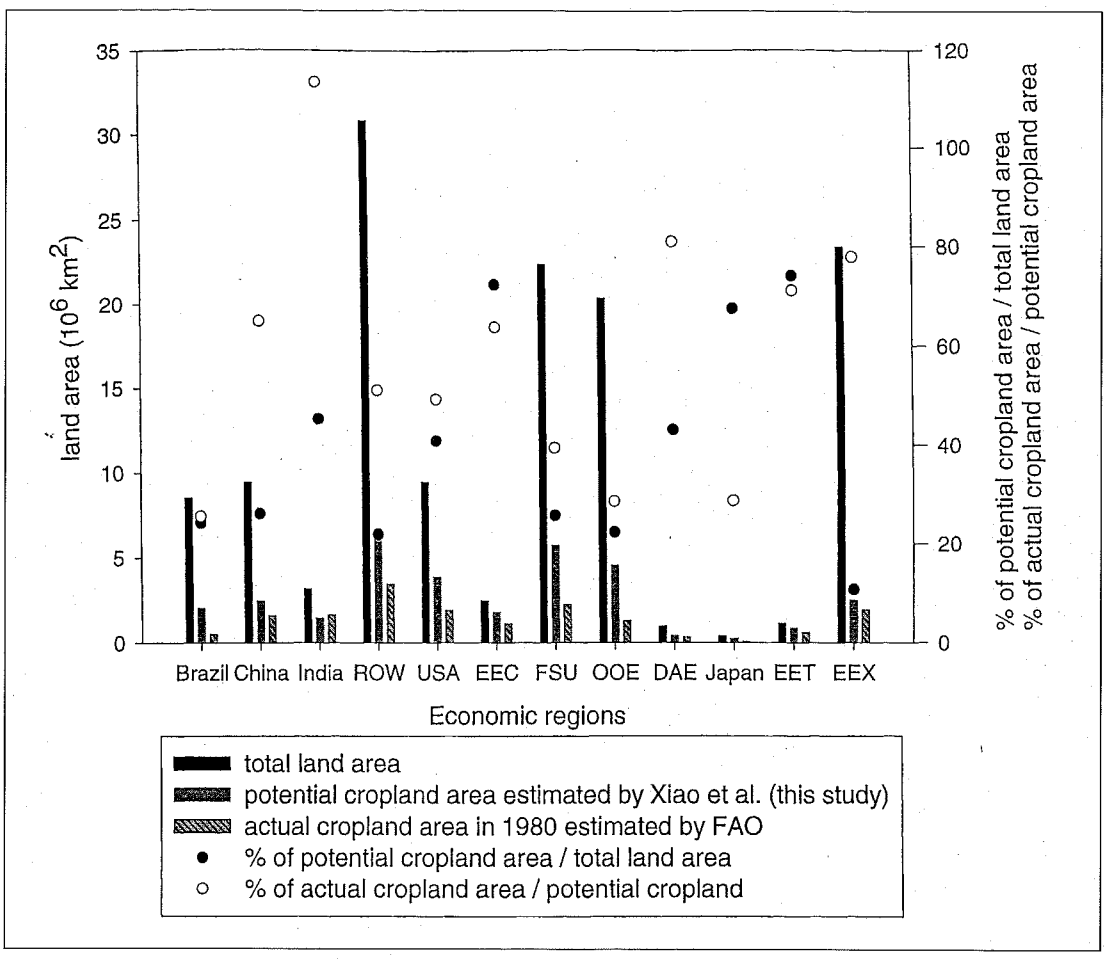

4. *Total land area, potential cropland area under contemporary climate, and actual cropland area in 1980 in the twelve economic regions of the world. These 12 economic regions are defined in the Anthropogenic Emission Prediction and Policy Analysis model (EPPA, Yang et al. 1996; Prinn et al. 1999): DAE – Dynamics Asian Economics, EEC - European Economic Community, EET - Eastern European Countries, EEX – Energy Exporting Countries, FSU – Former Soviet Union, OOE - the Other OECD Countries, ROW- the Rest of the World, USA – United States of America. Data of actual cropland area in 1980 are aggregated from the FAO country statistics data of agricultural production which are provided by Dr. G. Esser. Note that for Brazil, the ratio of potential cropland area over total land area is almost overlapped with the ratio of actual cropland area over potential cropland area*

irrigation from river water. The model also fails to project croplands in the semi-arid western United States where a large area of croplands is dependent on irrigation water from aquifers. The geographical distribution of potential croplands (fig. 5) is closely correlated with the geographical distribution of human population (fig. 6). Potential croplands occur mostly in those areas that have population densities of five or more people per square kilometer. Among the twelve economic regions, India and China have the highest population densities, indicating the highest pressure on potential croplands to be converted for crop cultivation. The cropland model estimates that large portions of moist tropical forests in Brazil, tropical Asian countries (e.g., Philippines, Indonesia and Malaysia) and Africa are not good for croplands due to the potential of severe soil erosion in croplands (fig. 5). In the map of Olson *et al.* (1983), there are only small areas of croplands in the moist tropical forests in Brazil but fair amounts of croplands in the tropical Asian countries where irrigated rice paddy dominates (fig. 5). The difference between Brazil and the tropical Asian countries may be attributed primarily to much higher population pressure for crop production in the tropical Asian countries from higher population density (more than 50 people per km^2, see fig. 6) and secondarily to monsoon climate in Asia. Our cropland distribution model estimates that a large portion of eastern Amazon is suitable for croplands (fig. 5), where extensive deforestation has been observed during the 1980s, with a fair portion of forest conversion to croplands and pasture. Skole and Tucker (1993) estimated that deforested area in Amazon is 78,000 km^2 in 1978 but 230,000 km^2 in 1988, using high resolution LANDSAT imageries. Deforestation in tropical regions is closely driven by increases of human population and other social-economic factors across local, regional, national and international levels (Fearnside 1993, Kummer and Turner 1994, Skole *et al.* 1994).

The effects of transient climate change on potential croplands

The cropland distribution model estimates that the area of global potential croplands increases under the three transient climate change predictions over the period of 1977 to 2100 (fig. 7). Compared to its value in 1977, the area of global potential croplands in 2100 increases about 11.6% (3.80 10^6 km^2) for the 'RRR', 12.6% (4.13 10^6 km^2) for the 'HHL', and 6.9% (2.25 10^6 km^2) for the 'LLH' transient climate change predictions, respectively. The projected area of global potential croplands under the 'HHL'

5. *The comparison between the map of croplands of Olson et al. (1983) and the map of global potential croplands under contemporary climate estimated by this cropland distribution model. In the map of croplands of Olson et al. (1983), both cultivation and secondary vegetation areas are included. Both maps have a spatial resolution of 0.5° latitude 0.5° longitude*

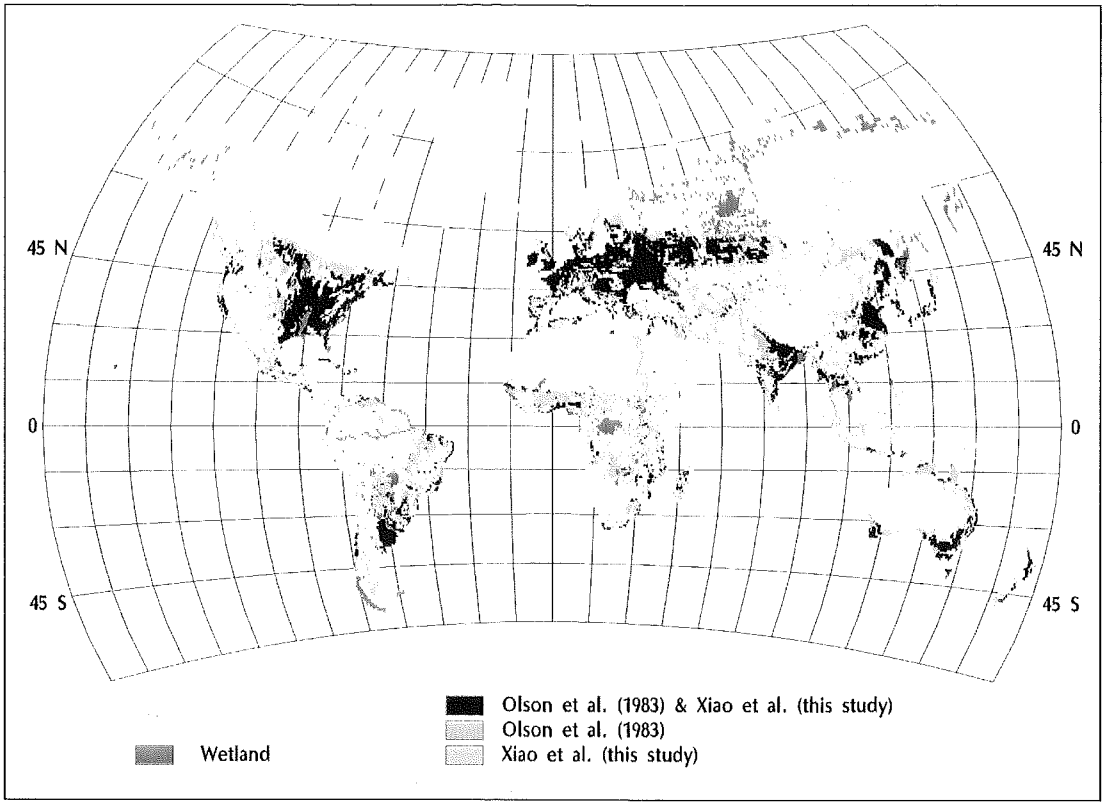

6. *Geographical distribution of population density (number of people per km2) of the world in 1994 at 0.5° latitude by 0.5° longitude resolution. It is aggregated from the Gridded Population of the World at 5 minute (latitude) by 5 minute (longitude) resolution, which is released by the Consortium for International Earth Science Information Network (CIESIN) and the National Center for Geographical Information and Analysis (NCGIA) in USA in 1995 (see Tobbler et al. 1995 and the web site http://www.ciesin.org). The unsmoothed population density data from the CIESIN and NCGIA are used and geographically cover areas from 57° S to 72° N*

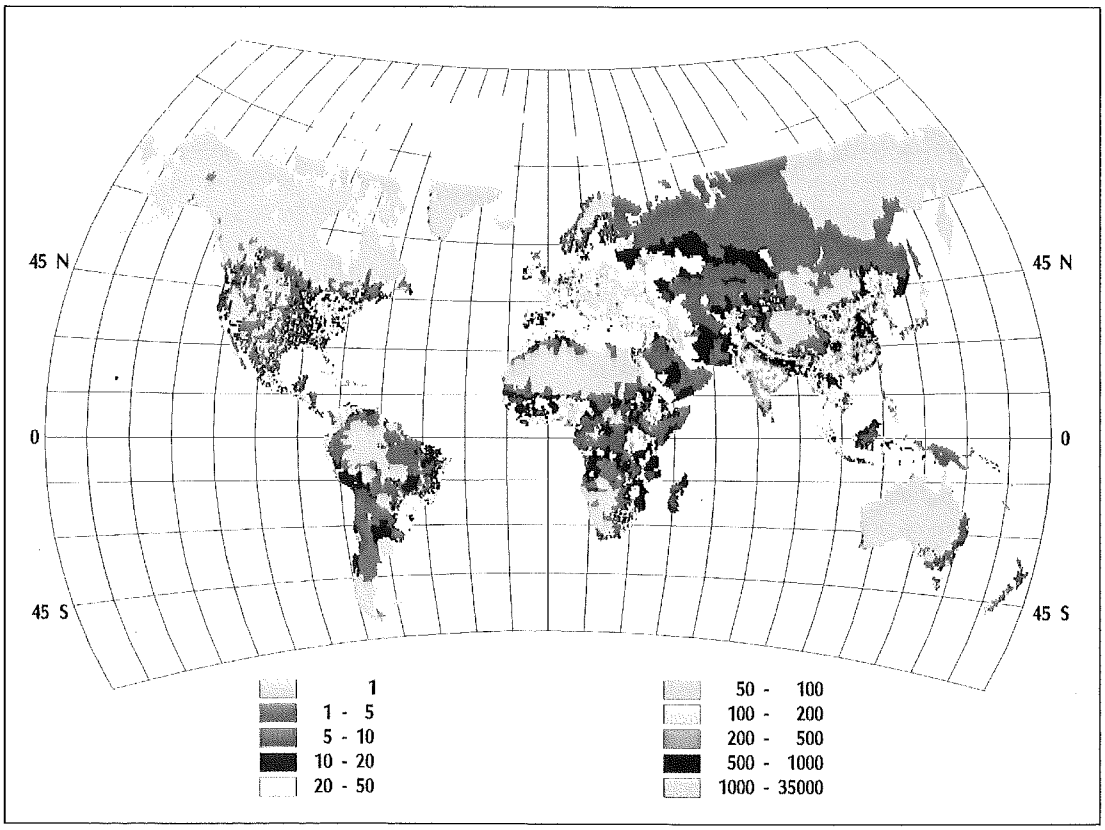

climate change prediction is only slightly higher than under the 'RRR' climate change prediction, although temperature changes in the 'HHL' scenario are much larger than in the 'RRR' scenario (fig. 3). In a modeling study using doubled CO_2 equilibrium climates from four GCMs (OSU, GISS, GFDL and UKMO), Cramer and Solomon (1993) estimated that the area of global potential croplands increases from about 18% under the OSU climate (smallest temperature increases) to about 38% under the UKMO climate (largest temperature increases). The difference in areal changes of global potential croplands between this study and Cramer and

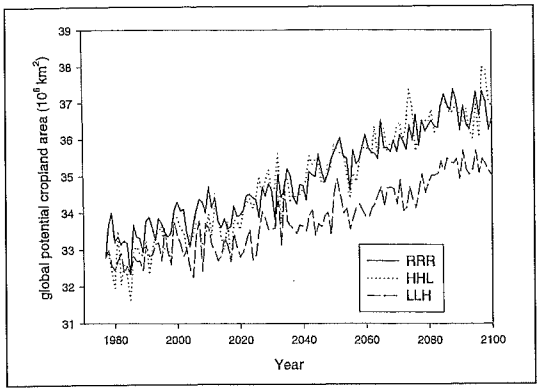

Solomon (1993) is partly due to the fact that this cropland distribution model has taken topographical constraints on cropland distribution into account.

The increase in global potential croplands is mostly attributable to the increases of potential croplands in the Former Soviet Union (FSU) and the Other OECD Countries (OOE) economic regions (fig. 8). In the Former Soviet Union the area of potential croplands in 2100 increases by 41% (2.37 10^6km^2) under the RRR, 48% (2.77 10^6 km^2) under the HHL and 26% (1.52 10^6km^2) under the LLH predictions. In the Other OECD Countries region the area of potential croplands in 2100 increases by 32% (1.44 10^6km^2) under the RRR, 33% (1.51 10^6km^2) under the HHL and 19% (0.85 10^6 km^2) under the LLH predictions. The United States of America (USA) has a slight increase of potential cropland by the end of 21st century (fig. 8). However, China and India may have small decreases in the area of potential croplands by the end of 21st century. In 2100 the area of potential croplands in China reduces by 4% (0.09 10^6km^2) under the RRR, 6% (0.14 10^6 km^2) under the HHL and 2% (0.04 10^6km^2) under the LLH climate change predictions. The other eight economic regions have little changes in areas of potential croplands. The relative contributions from each of the twelve economic regions to the increase of global potential croplands are similar among these three transient climate change predictions (fig. 8).

Geographically, there exist an expansion of potential croplands and a reduction of potential croplands under the three transient climate change predictions (figs. 10, 11, 12). Compared to its value in 1977, there is an expansion of 16% (5.37 10^6 km^2) new potential croplands and a reduction of 5% (1.57 10^6 km^2) potential croplands in 2100 under the RRR climate change prediction (fig. 10). Similarly, an expansion of potential croplands in 2100 is about 17% (5.70 10^6 km^2) under the HHL and about 11% (3.63 10^6 km^2) under the LLH climate change predictions, and a reduction of potential croplands in 2100 reaches about 5% (1.57 10^6 km^2) under the HHL and about 4%

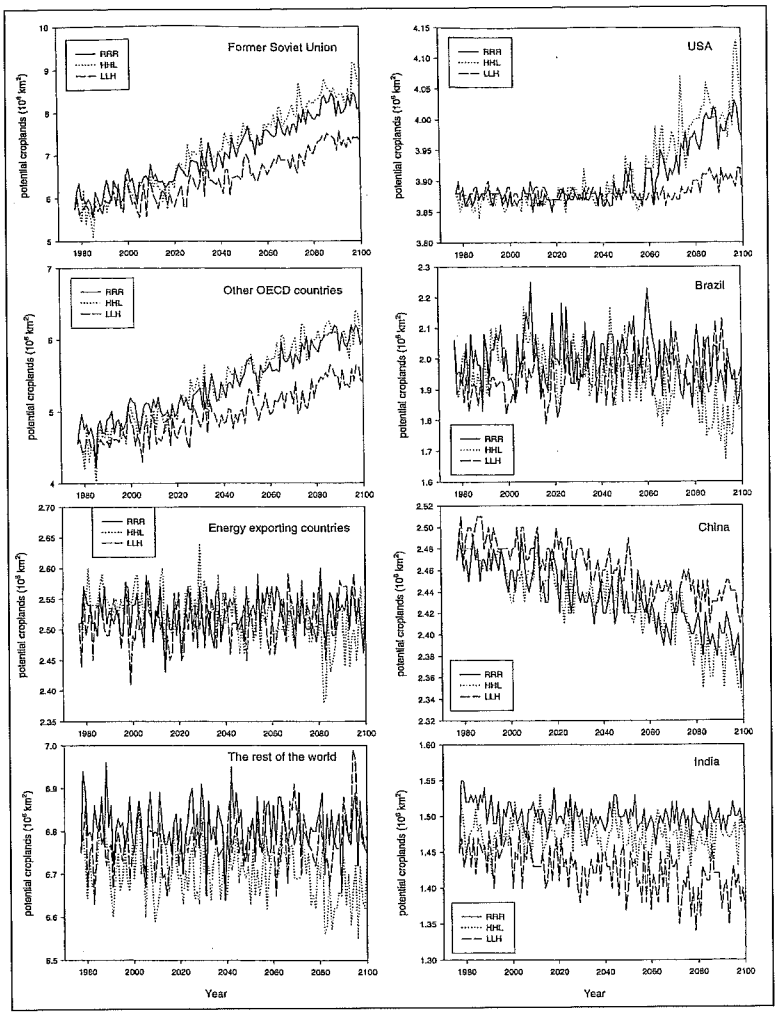

(1.39 10^6 km^2) under the LLH climate change predictions. The expansions of potential croplands occur mostly in high latitudes of the Northern Hemisphere (figs. 10, 11, 12). The northward expansion of potential croplands is largest in the 'HHL' but lowest in the 'LLH' climate change predictions. Russia and Canada have the largest increases in potential cropland area, which is mostly attributed to large temperature increases in high latitudes. The 2-D land-ocean climate projected a larger temperature increase in high latitudes than in low latitudes (Prinn *et al.* 1999), which is consistent with the results of 3-D GCMs (Mitchell *et al.* 1990). Kazakhstan, Uzbekistan and Turkmenistan in the Former Soviet Union economic region have a large expansion of potential croplands and also a large reduction of potential croplands (figs. 10, 11, 12). A moderate reduction of potential croplands occurs in the Southern America, Australia and China (figs. 10, 11, 12).

7. *Temporal changes in the area of global potential croplands over the period of 1977-2100 under the RRR, HHL and LLH climate change predictions*

8. *Temporal changes in the areas of potential croplands in the eight economic regions over the period of 1977-2100 under the RRR, HHL and LLH transient climate change predictions*

Discussion

The 2-D land-ocean climate model projects much smaller spatial variation in climate than the 3-D ocean-atmosphere GCMs, because it has no

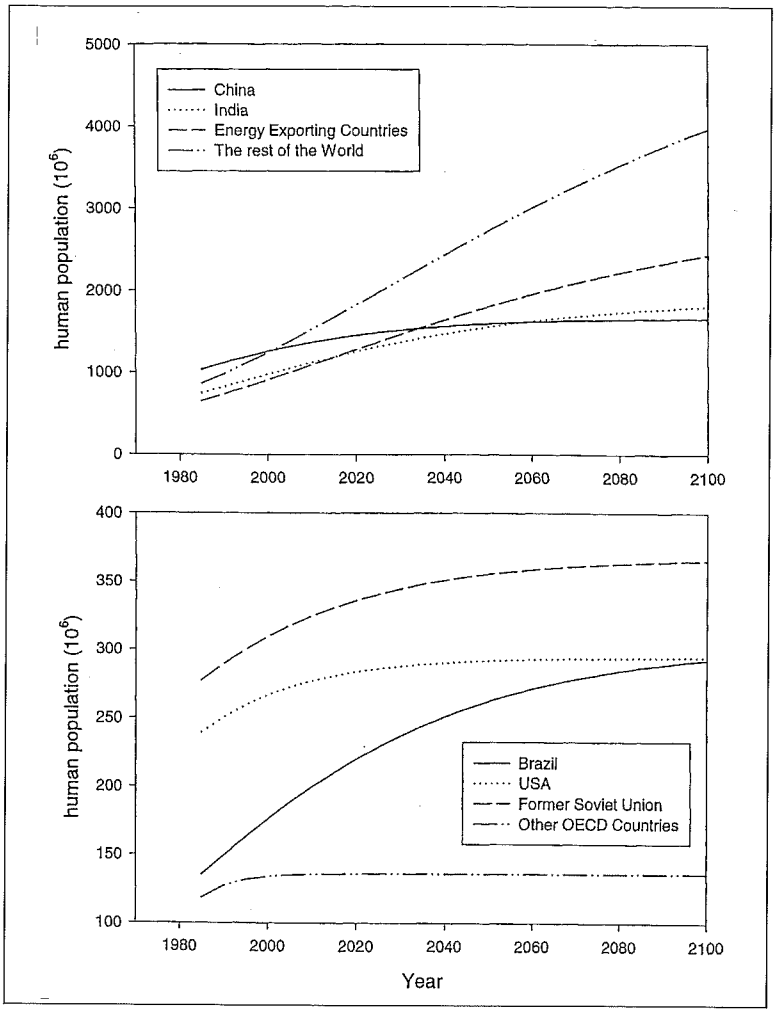

9. *Temporal changes of human population in the eight economic regions over the period of 1985 - 2100. These projections by the Anthropogenic Emission Prediction and Policy Analysis model (EPPA, Yang et al. 1996) are based on the estimates of United Nations (see Bulatao et al. 1990)*

variation among the grid cells along a longitude band. A number of 3-D ocean-atmosphere GCMs have simulated transient climate changes over time (Kattenberg *et al.* 1996), it would be useful to use them to drive the cropland distribution model to examine the effects of both longitude and latitude variations in climate change on potential croplands. Also note that the interannual variation of climate projected by the 2-D land-ocean climate model (fig. 3) is much smaller than the observed interannual variation of climate in the last few decades (see Dai and Fung, 1993), being about half of interannual variation of climate projected by the coupled ocean-atmosphere general circulation models (GCMs) (Sokolov and Stone 1998). The results of this study still show large interannual variations in the area of global potential croplands over the period of 1977-2100 due to interannual variation of climate (fig. 7). Therefore, if driven by transient climate change predictions of 3-D GCMs, the cropland distribution model may give much larger spatial and temporal variations in global potential croplands. However, these coupled atmospheric-ocean GCMs experiments (Kattenberg *et al.* 1996) were driven by only one transient scenario of CO_2 change over time, and most of them used 1% CO_2 increase per year over time. In order to quantify the sensitivity and uncertainty of cropland responses to transient climate change in the 21st century, a significant number of transient climate change simulations associated with various scenarios of anthropogenic emissions of greenhouse gases is required.

The comparison in geographical distributions between potential croplands (fig. 5) and human population (fig. 6) indicates that further studies are needed to quantify the relationship between cropland distribution and spatial distribution of human population on the global scale. Human population is likely to increase substantially in developing countries, e.g., China, India, Brazil, Energy Exporting Countries and the Rest of the World economic regions, while developed countries (e.g., USA, the Other OECD Countries and the Former Soviet Union economic regions) are likely to have small increases of population (fig. 9). This study has shown that transient climate change can significantly affect the area and spatial distribution of potential croplands of the world over the period of 1977-2100. Developed countries account for most of the projected increases in global potential croplands, while developing countries have little changes in the areas of potential croplands. For developing countries, opposite trends in population and potential cropland area indicate an increasing pressure to raise agricultural production per unit area. These developing countries, however, are under the largest constraints in energy and resources, which are essential for intensive agricultural production. Future climate change and an increase of atmospheric CO_2 concentration are also likely to affect crop production significantly (Reilly 1996, Wittwer 1995, Rosenzweig and Parry 1994). In a recent study which uses comparable crop yield models with doubled CO_2 equilibrium climate changes from three GCMs (GISS, GFDL, UKMO) to assess the potential impacts of climate change on world food supply, the results suggest that doubling of pre-industrial atmospheric CO_2 concentration will lead to a small decrease in global crop production (Rosenzweig and Parry 1994). Climate change increases cereal production per hectare in the developed countries but reduces cereal production per hectare in developing countries (Rosenzweig and Parry 1994). One important implication from the comparison among population dynamics, potential cropland area and crop production per hectare is that international trade in agricultural products will have to be substantially increased between developed countries and developing countries in order to avoid food shortage in some countries in the 21st century.

In this study, the cropland distribution model projects a northward expansion of potential

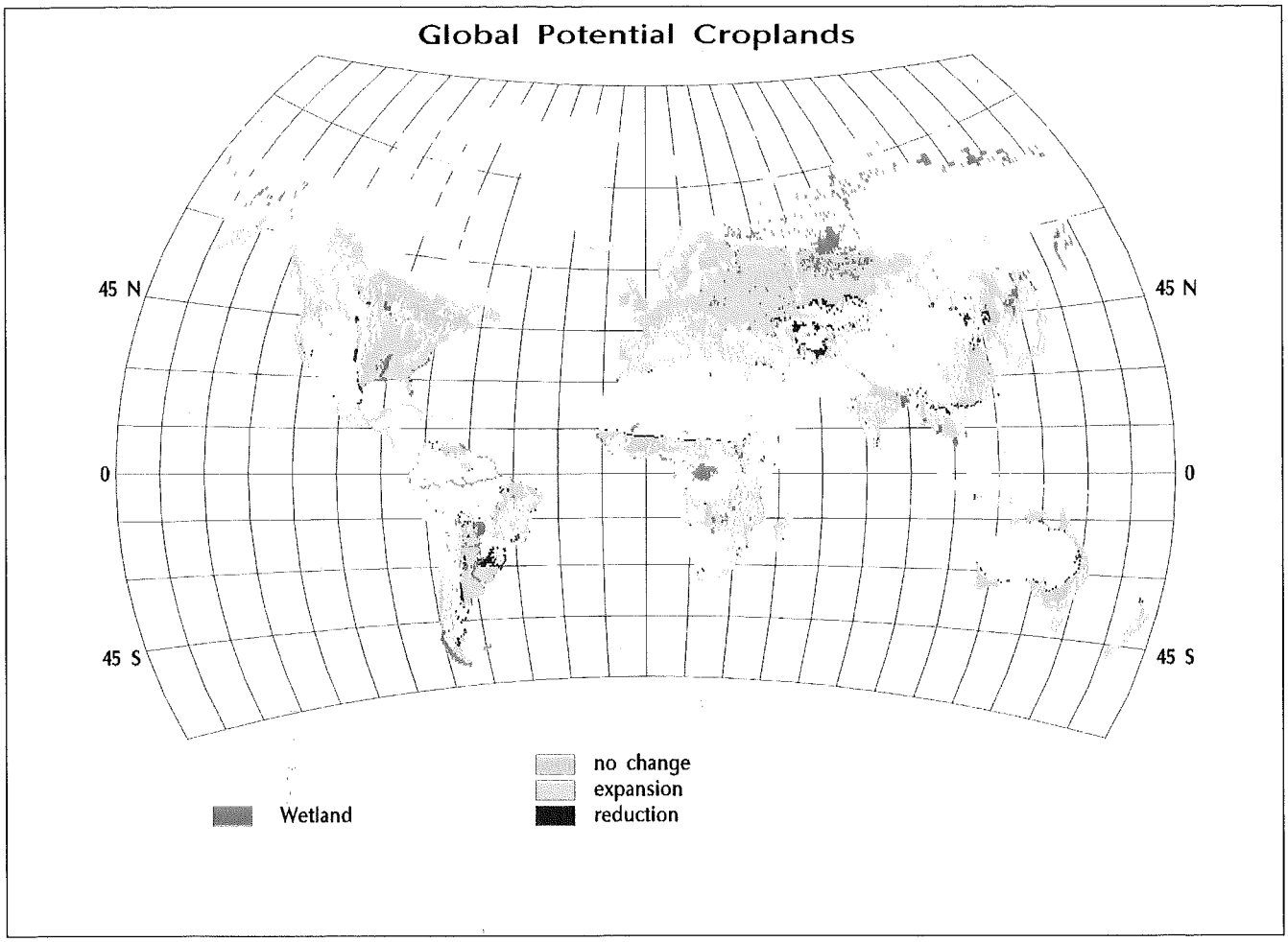
Global Potential Croplands
45 N
0
45 S
45 N
0
45 S
no change
expansion
reduction
Wetland

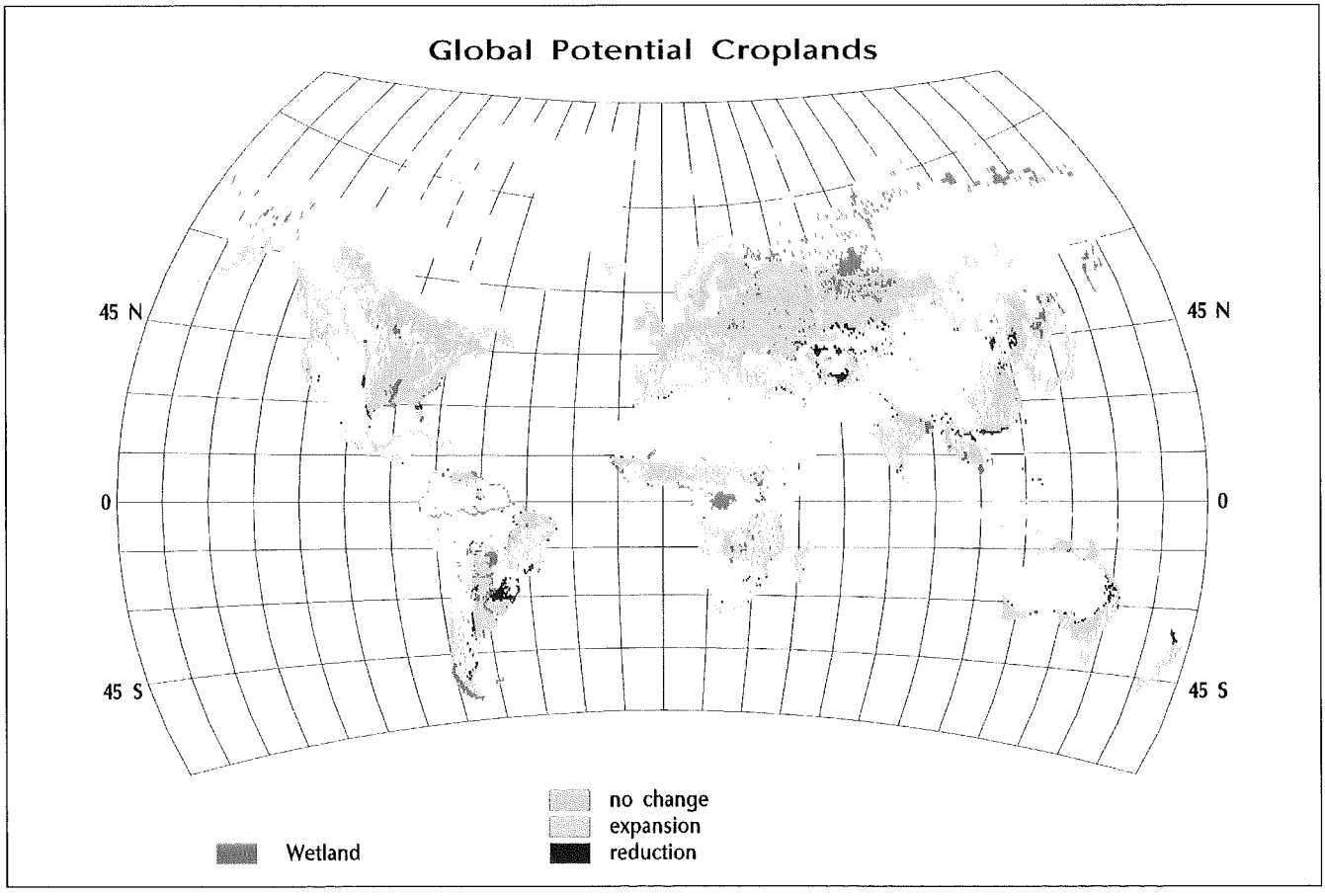
Global Potential Croplands
45 N
0
45 S
45 N
0
45 S
no change
expansion
reduction
Wetland

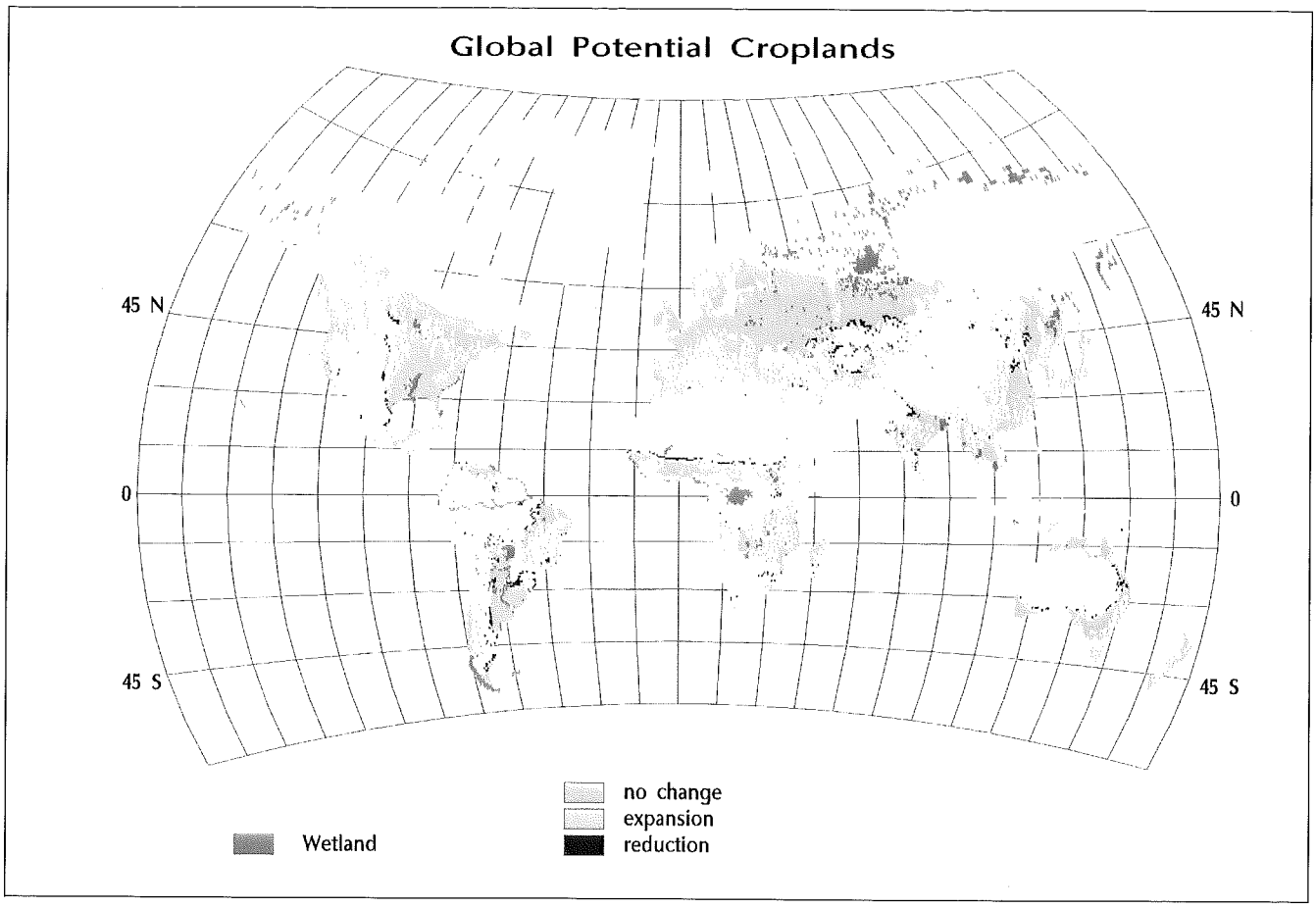

On page 105

10. *Changes in spatial distribution of global potential croplands between year 2100 and the contemporary climate under the RRR transient climate change prediction*

11. *Changes in spatial distribution of global potential croplands between year 2100 and the contemporary climate under the HHL transient climate change prediction*

On this page

12. *Changes in the spatial distribution of global potential croplands between year 2100 and the contemporary climate under the LLH transient climate change prediction*

croplands into high latitudes in the 21st century under the three transient climate change predictions. Cramer and Solomon (1993) also projected a northward expansion of potential croplands into high latitudes under the doubled CO_2 equilibrium climates projected by the four GCMs (OSU, GISS, GFDL and UKMO). However, in high latitudes where tundra and boreal forests dominate, large portions of soils are spodosols and histosols. Soil physical (e.g., water-saturation in histosols) and chemical properties (e.g., pH, cation exchange capacity) of these soils may also constrain distribution of croplands, therefore, large amounts of additional resources and inputs (e.g., drainage, lime application) are needed to change soil physical and chemical properties so that soils is suitable for crop cultivation.

The potential expansion of croplands into high latitudes in the Northern Hemisphere in the 21st century may have significant impacts on global carbon budget. As simulated by a global biogeochemistiry model (Terrestrial Ecosystem Model (TEM), Xiao *et al.* 1997), total carbon storage (vegetation carbon plus reactive soil organic carbon) under contemporary climate at 315 ppmv CO_2 has a bimodal distribution along 0.5° latitudinal bands (fig. 13). Of 1658.6 PgC (10^{15} g C) total carbon storage of the terrestrial biosphere (Xiao *et al.* 1997), 423.6 PgC (25.5%) is stored within the tropical latitudes (10°S - 10°N) where tropical forests dominate, and 420.8 PgC (25.4%) is stored within the 45°N - 65°N, where boreal forests and tundra dominate. In tropical forest ecosystems, vegetation carbon is substantially higher than reactive soil organic carbon, while a large portion of carbon in boreal forests and tundra ecosystems is stored in soils. In calculating the effects of land cover and land use changes on the historical and present global carbon budget (Esser 1987, Houghton 1996), tropical deforestation plays a dominant role in CO_2 emissions from land use and land cover changes. Conversion of boreal forests and tundra into croplands may also result in a large loss of carbon in vegetation and soils, and will affect carbon flux and storage in the terrestrial biosphere. Our study implies that the effort to stabilize atmospheric CO_2 concentration in the next centuries may also need to take into consideration of the constraints of land use and land cover changes at mid- to high- latitudes of the Northern Hemisphere.

This version of cropland distribution model, which is currently based on climate, soil and topography, evaluates suitability of land potential for agricultural production and provides the area and spatial distribution of potential croplands in the world under the contemporary climate. The resulted information is essential for modeling

spatial distribution and dynamics of actual croplands in the world. The United Nations Food and Agriculture Organization (FAO) provides country statistics of agriculture, for instance, approximately 15 10^6 km^2 area was actually growing crops in 1984 (FAO 1986). The International Geosphere-Biosphere Program (IGBP) Data and Information System (DIS) recently used monthly normalized difference vegetation index (NDVI) data derived from the NOAA AVHRR satellite at 1-km spatial resolution from April 1992 to March 1993 to generate a global data set of land cover types (Loveland and Belward 1997). The IGBP-DIS estimated that there were 14.02 10^6 km^2 of croplands and 13.94 10^6 km^2 area of cropland/natural vegetation mosaic, i.e., a total area of 27.96 10^6 km^2. This satellite-derived cropland data set provides a new opportunity to re-examine the relationship between croplands and climate on the scales of the global and continents (e.g., monsoon climate in the Asia). The cropland distribution model could be further improved to provide better estimates of potential croplands in the world. For example, the global extrapolation of the cropland distribution model in this study has a spatial resolution of 0.5° (longitude) 0.5° (latitude), which cannot account for large subgrid variations of land cover and land use, especially in mountainous regions. Extrapolation of the cropland distribution model at much finer spatial resolutions (e.g., 5' longitude by 5' latitude or 1 km by 1 km) may improve evaluation and estimate of potential croplands in the world if global data of climate, vegetation, soil and elevation at such finer spatial resolutions become available in the near future. The incorporation of a global large river network into the cropland distribution model may improve the estimate of potential croplands under contemporary climate and provide a basis to assess the effects of water supply (particularly in semi-arid and arid regions) on agriculture in the future. Further work is also needed to model or delineate spatial distributions of various major crops on the globe (Leemans and Solomon 1993). The information on potential croplands would be one of many inputs (e.g., human population and other socioeconomic factors) for land use models to determine the area and spatial distribution of actual croplands on the globe. The dynamic linkage of a land cover and land use change model, a global terrestrial biogeochemistry model (e.g, TEM) and a climate model will allow us to assess the impacts of land cover and land use change on global terrestrial carbon and nitrogen cycling as well as atmosphere composition and climate over time.

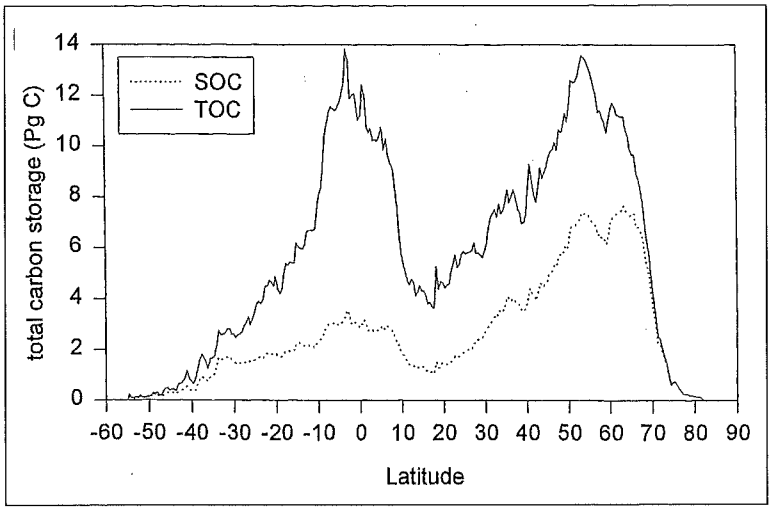

13. *Latitudinal distribution of total carbon storage (TOC) and reactive soil organic carbon (SOC) for the contemporary climate with 315 ppmv CO_2 along 0.5° resolution latitudinal bands, as estimated by the Terrestrial Ecosystem Model (see Xiao et al. 1997). Total carbon storage estimated by TEM is the sum of vegetation carbon and reactive soil organic carbon. Estimates of reactive soil organic carbon in a grid cell exclude inert soil organic carbon. Vegetation carbon is the difference between total carbon storage (TOC) and reactive soil organic carbon (SOC)*

Acknowledgments

We thank B.L. Turner II, R.G. Prinn, J.D. Henry and R. Eckaus for invaluable discussion and comments on the work and earlier versions of the manuscript. G. Esser provides actual cropland data at country level in 1980 from FAO. This study was completed in 1997 while X. Xiao was working at the Ecosystems Center, Marine Biological Laboratory, Woods Hole, Massachusetts. This study was supported by the Joint Program on the Science and Policy of Global Change at Massachusetts Institute of Technology (CE-S-462041), National Institute of Global Environmental Changes of Department of Energy (No: 901214-HAR) and Earth Observing Systems Program of NASA (NAGW-2669). Updated version for *Sistema Terra: Remote Sensing and the Earth*

Bibliography

Beniston, M. and Fox, D.G. 1996. Impacts of Climate Change on Mountain Regions. In: *Climate Change 1995 - Impacts, Adaptations and Mitigation of Climate Change: Scientific-Technical Analyses.* Contribution of Working Group II to the Second Assessment Report of the Intergovernmental Panel on Climate Change. Watson, R.T., Zinyowera, M.C., Moss, R.H. and Dokken, D.J. (eds.). Cambridge University Press, pp. 191-213.

Bradbury, I., Kirkby, R. and Shen, G. 1996.Development and Environment: the case of rural industrialization and small-town growth in China. *Ambio* 25, 204-209.

Brinkman, R. 1987. Agro-ecological Characterization, Classification and Mapping: Different approaches by the International Agricultural Centers. In: Bunting, A.H. (ed.) *Agricultural Environments.Characterization,Classification and Mapping.* C.A.B. International, Wallingford, U.K. pp. 31-42.

Bulatao, R.A., Bos, E., Stephens, P.W.S. and Vu, M.T. 1990. *World Bank Population Projections 1989-1990 Edition.* John Hopkins University Press, Baltimore.

Bullock, P. and Le Houerou, H. 1996. Land degradation and Desertification. In: *Climate Change 1995 - Impacts, Adaptations and Mitigation of Climate Change: Scientific-Technical Analyses.* Contribution of Working Group II to the Second Assessment Report of the Intergovernmental Panel on Climate Change. Watson, R.T., Zinyowera, M.C., Moss, R.H. and Dokken, D.J. (eds.). Cambridge University Press, pp. 171-189.

Cramer, W.P. and Solomon, A.M. 1993. Climatic classification and future global redistribution of agricultural land. *Climate Research* 3, 97-110.

Dai, A. and I.Y. Fung. 1993. Can Climate Variability Contribute to the 'Missing' CO2 sink? *Global Biogeochemical Cycles* 7, 599-609.

Douglas, I. 1994. Human settlements. In: *Changes in Land Use and Land Cover: A Global Perspective.* Meyer, W.B. and Turner II, B.L. (eds.). Cambridge University Press, New York, pp. 149-169.

Esser, G. 1987. Sensitivity of Global Carbon Pools and Fluxes to Human and Potential Climatic Impacts. *Tellus* 39B, 245-60.

FAO. 1978. *Report on the Agro-Ecological Zone project.* Vol. 3. Methodology and Results for South and Central America. World Soil Resources Report 48/3. FAO, Rome.

FAO. 1980. *Production Yearbooks*, Vol. 33. FAO Statistics Series No. 28. Food and Agricultural Organization of the United Nations, Rome.

FAO. 1986. *1985 FAO Production Yearbook*, Vol. 39. Food and Agricultural Organization of United Nations, Rome.

FAO/IIASA. 1993. Agro-ecological Assessments for National Planning: the Examples of Kenya. *FAO Soils Bulletin* 67. FAO, Rome.

FAO-UNESCO. 1971. *Soil map of the world*, scale 1:5,000,000. UNESCO, Paris, France. Digitization at 0.5°-resolution by Complex Systems Research Center, University of New Hampshire, Durham, and modifications by Marine Biological Laboratory, Woods Hole.

Fearnside, P.M. 1993. Deforestation in Brazilian Amazonia: the effect of population and land tenure. *Ambio* 22, 537-545.

Grübler, A. 1994. Technology. In: *Changes in Land Use and Land Cover: A Global Perspective.* In: Meyer, W.B. and Turner II, B.L. (eds.). Cambridge University Press, New York, pp. 287-328.

Houghton, R.A. 1996. Terrestrial Sources and Sinks of Carbon Inferred from Terrestrial Data. *Tellus* 48B, 420-432.

IPCC. 1994. *Climate Change 1994: Radiative Forcing of Climate Change and an Evaluation of the IPCC IS92 Emission Scenarios.* Intergovernmental Panel on Climate Change. Cambridge University Press, pp. 233-304.

Jensen, M.E. and Haise, H.E. 1963. Estimating Evapotranspiration from Solar Radiation.
Journal of the Irrigation and Drainage Division 4, 15-41.

Kattenberg, A., Giorgi, F., Grassl, H., Meehl, G.A., Mitchell, J.F.B., Stouffer, R.J., Tokioka, T., Weaver, A.J. and Wigley, T.M.L. 1996. Climate Models – Projections of future climate. In: *Climate Change 1995: The Science of Climate Change.* Houghton, J.T., Meira Filho, L.G., Callander, B.A., Harris, N., Kattenberg, A. and Maskell, K. (eds.). Intergovernmental Panel on Climate Change, Cambridge University Press, pp. 284-357.

Kummer, D.M. and Turner II, B.L. 1994. The human Causes of Deforestation in Southeast Asia. *Bioscience* 44, 323-328.

Leemans, R. and Cramer, W.P. 1991. The IIASA climate database for land areas on a grid with 0.5° resolution *Research Report* RR-91-18, International Institute for Applied Systems Analysis (IIASA), Laxenburg, Austria. 60 p.

Leemans, R. and Solomon, A.M. 1993. Modeling the Potential Change in Yield and Distribution of the Earth's Crops under a Warmed Climate. *Climate Research* 3, 79-96.

Liu, Y. 1996. Modeling the Emission of Nitrous Oxide (N2O) and Methane (CH4) from the Terrestrial Biosphere to the Atmosphere. MIT Joint Program on the Science and Policy of Global Change, *Report* 10, 219 pages. Massachusetts Institute of Technology, Cambridge, MA, August 1996. Ph. D. Dissertation.

Loveland, T.R. and Belward, A.S., 1997. The IGBP-DIS global 1-km land cover data set, DISCover: first results. *Int. J. Remote Sensing*, 18: 3289-3295.

Matthews, E. 1983. Global vegetation and Land Use: new high resolution databases for climate studies. *J. Climatol. Appl. Meteorol.* 22, 474-487.

McGuire, A.D., Melillo, J.M., Kicklighter, D.W., Pan, Y., Xiao, X., Helfrich, J., Moore III, B., Vörösmarty, C.J. and Schloss, A.L. 1997. Equilibrium Responses of Global Net Primary Production and Carbon Storage to Doubled Atmospheric Carbon Dioxide: Sensitivity to Changes in Vegetation Nitrogen Concentration. *Global Biogeochemical Cycles* 2: 173-189.

Melillo, J.M., McGuire, A.D., Kicklighter, D.W., Moore III, B., Vörösmarty, C.J. and Schloss, A.L. 1993. Global Climate Change and Terrestrial Net Primary Production. *Nature 363*: 234-240.

Mitchell, J.F.B., Manabe, S., Tokioka, T. and Meleshko, V., 1990. Equilibrium Climate Change and its Implications for the future. In: Houghton, J.T., Jenkins, G.J., and Ephraums, J.J. (eds.) *Climate Change: The IPCC Scientific Assessment.* Cambridge University Press, New York. pp. 131-164.

Naylor, R.L. 1996. Energy and Resource Constraints on Intensive Agricultural Production. *Annual Review of Energy and Environment.* 21, 99-123.

NCAR/NAVY. 1984. *Global 10-minute elevation data.* Digital tape available through National Oceanic and Atmospheric Administration, National Geophysical Data Center, Boulder.

Olson, J.S., Watts, J.A. and Allison, L.J. 1983. *Carbon in Live Vegetation of Major World Ecosystems.* ORNL 5862. Oak Ridge National Laboratory, Oak Ridge, TN.

Prinn, R., Jacoby, H., Sokolov, A., Wang, C., Xiao, X., Yang, Z., Eckaus, R., Stone, P., Ellerman, D., Melillo, J., Fitzmaurice, J., Kicklighter, D., Holian, G., and Liu, Y., 1999. Integrated Global System Model for Climate Policy Assessment: Feedbacks and Sensitivity Studies, *Clim. Change*, 41: 469-546.

Raich, J.W., Rastetter, E.B., Melillo, J.M., Kicklighter, D.W., Steudler, P.A., Peterson, B.J., Grace, A.L., Moore III, B. and Vörösmarty, C.J., 1991. Potential Net Primary Productivity in South America: application of a global model. *Ecological Applications* 1, 399-429.

Reilly, J. 1996. Agriculture in a Changing Climate: Impacts and adaptation. In: *Climate Change 1995 - Impacts, Adaptations and Mitigation of Climate Change: Scientific-Technical Analyses.* Contribution of Working Group II to the Second Assessment Report of the Intergovernmental Panel on Climate Change. Watson, R.T., Zinyowera, M.C., Moss, R.H. and Dokken, D.J. (eds.). Cambridge University Press, pp. 427-467.

Rosenzweig, C. and Parry, M.L. 1994. Potential Impact of Climate Change on World Food Supply. *Nature* 367, 133-138.

Skole, D.L., and Tucker, C.J. 1993. Tropical Deforestation and Habitat Fragmentation in the Amazon: Satellite data from 1978 to 1988. *Science* 260, 1905-1910.

Skole, D.L., Chomentowski, W.H., Salas, W.A. and Nobre, A.D. 1994. Physical and Human Dimensions of Deforestation in Amazonia. *Bioscience* 44, 314-322.

Sloss, P.W. 1996. Enhancing NOAA's Image: Imagery in print, on walls and on the World Wide Web. *Earth System Monitor* 7(1), 1-2. September 1996.

Sokolov, A.P. and Stone, P.H. 1995. Description and Validation of the MIT Version of the GISS 2-D Model. MIT Joint Program on the Science and Policy of Global Change *Report* 2. Massachusetts Institute of Technology. 46 pp.

Sokolov, A.P. and Stone, P.H., 1998. A Flexible Climate Model for Use in Integrated Assessments, *Climate Dynamics*, 14, 291-303.

Stone, P.H. and Yao, M.S. 1987. Development of a Two-Dimensional zonally averaged Statistical-dynamical Model. Part II. The role of eddy momentum fluxes in the general circulation and their parameterization. *Journal of the Atmospheric Science 44(24)*, 3769-3786.

Stone, P.H. and Yao, M.S. 1990. Development of a Two-Dimensional Zonally averaged Statistical-dynamical Model. Part III. The parameterization of the eddy fluxes of heat and moisture. *Journal of Climate 3(7)*, 726-740.

Tobler, W., Deichmann, U., Gottsegen, J. and Maloy, K. 1995. The Global Demography Project. National Center for Geographical Information and Analysis *Technical Report* TR-96-6. Department of Geography, University of California, Santa Barbara, CA 93106.

Vörösmarty, C.J., Moore III, B., Grace, A.L., Gildea, M.P., Melillo, J.M., Peterson, B.J., Rastetter, E.B. and Steudler, P.A., 1989. Continental Scale Models of Water Balance and Fluvial Transport: An application to South America. *Global Biogeochemical Cycle 3(3)*, 241-265.

Wang, C., Prinn, R.G., Sokolov, A., Stone, P.H., Liu, Y. and Xiao, X., 1995. A Coupled Atmospheric Chemistry and Climate Model for Chemically and radiatively important Trace Species. WMO-IGAC Conference on the Measurement and Assessment of Atmospheric Composition Change, 9-14 October 1995, Beijing; WMO GAW No. 107: 182-184

Wang, C., R.G. Prinn, and A. Sokolov, A Global Interactive Chemistry and Climate Model: Formulation and testing, *J. Geophys. Res.*, 103, 3399-3417, 1998.

Wittwer, S.H. 1995. *Food, Climate and Carbon Dioxide: The Global Environment and World Food Production.* Lewis Publishers, New York, 236 p.

World Resource Institute. 1992. *World Resources 1992-1993.* Oxford University Press, Oxford, UK. 385

Xiao, X., Kicklighter, D.W., Melillo, J.M., McGuire, A.D., Stone, P.H. and Sokolov, A.P., 1997. Linking a Global Terrestrial Biogeochemical Model and a 2-dimensional Climate Model: Implications for the global carbon budget. *Tellus* 49B, 18-37.

Xiao, X., Melillo, J.M., Kicklighter, D.W., McGuire, A.D., Prinn, R.G., Wang, C., Stone, P.H. and Sokolov, A.P., 1998. Transient Climate Change and Net Ecosystem Production of the Terrestrial Biosphere. *Global Biogeochemical Cycles*, 2: 345-360.

Yang, Z., Eckaus, R.S., Ellerman, A.D., Fitzmaurice, J. and Jacoby, H.D., 1996. The MIT Emission Prediction and Policy Analysis (EPPA) model. MIT Joint Program on the Science and Policy of Global Change, *Report* No. 6. 49 pages. Massachusetts Institute of Technology, Cambridge, MA, June 1996.

Yao, M.S. and Stone, P.H. 1987. Development of a Two-Dimensional zonally averaged Statistical-Dynamical Model. Part I: The parameterization of moist convection and its role in the general circulation. *Journal of the Atmospheric Sciences 44(1)*, 65-8.

On pages 94-95 Space Radar Image of Namibia Sand Dunes

This spaceborne radar image shows part of the vast Namib Sand Sea on the west coast of southern Africa, just northeast of the city of Luderitz, Namibia. The magenta areas in the image are fields of sand dunes, and the orange area along the bottom of the image is the surface of the South Atlantic Ocean. The region receives only a few centimeters (inches) of rain per year. In most radar images, sandy areas appear dark due to their smooth texture, but in this area the sand is organized into steep dunes, causing bright radar reflections off the dune "faces." This effect is especially pronounced in the lower center of the image, where many glints of bright radar reflections are seen. Radar images of this hyper-arid region have been used to image sub-surface features, such as abandoned stream courses. The bright green features in the upper right are rocky hills poking through the sand sea. The peninsula in the lower center, near Hottentott Bay, is Diaz Point; Elizabeth Point is south of Diaz Point.

This image was acquired by Spaceborne Imaging Radar-CIX-Band Synthetic Aperture Radar (SIR-CIX-SAR) onboard the space shuttle Endeavour on April 11, 1994. The image is 54.2 kilometers by 82.2 kilometers (33.6 miles by 51.0 miles) and is centered at 26.2 degrees South latitude, 15.1 degrees East longitude. North is toward the upper left. The colors are assigned to different radar frequencies and polarizations of the radar as follows: red is L-band, horizontally transmitted and received; green is L-band, horizontally transmitted, vertically received; and blue is C-band, horizontally transmitted, horizontally received. SIR-CIX-SAR, a joint mission of the German, Italian, and United States space agencies, is part of NASA's Mission to Planet Earth.

MIT JOINT PROGRAM ON THE SCIENCE AND POLICY OF GLOBAL CHANGE
REPRINT SERIES

Joint Program Reprints are available free of charge (limited quantities.) To order: please use contact information on inside of front cover.

JP 99-008. Obstacles to global CO_2 trading: A familiar problem, A.D. Ellerman, *Climate Change Policy: Practical Strategies to Promote Economic Growth and Environmental Quality,* pp. 119–32, May 1999. American Council for Capital Formation Center for Policy Research, Washington, D.C. (Also JP Report No. 42)

JP 99-009. Tradable emissions rights and Joint Implementation for greenhouse gas abatement: A look under the hood, R. Schmalensee, pp. 39–55, with Commentary by R.G. Prinn, pp. 65–71, in *The Impact of Climate Change Policy on Consumers: Can Tradable Permits Reduce the Cost?* April 1998. American Council for Capital Formation Center for Policy Research, Washington, D.C.

JP 99-010. The role of science in policy: The climate change debate in the United States, E. Skolnikoff, *Environment* 41(5): 16–20, 42–45, June 1999. (Also JP Report No. 46)

JP 99-011. Impact of emissions, chemistry and climate on atmospheric carbon monoxide: 100-yr predictions from a global chemistry-climate model, C. Wang and R.G. Prinn, *Chemosphere: Global Change Science* 1 (1-3): 73-81(1999). (Also JP Report No. 35)

JP 99-012. Multi-gas assessment of the Kyoto Protocol, J. Reilly, R. Prinn, J. Harnisch, J. Fitzmaurice, H. Jacoby, D. Kicklighter, J. Melillo, P. Stone, A. Sokolov, and C. Wang, *Nature* 401: 549-55, October 1999. (Also JP Report No. 45)

JP 99-013. Agricultural impact assessment, vulnerability, and the scope for adaptation, J.M. Reilly and D. Schimmelpfennig, *Climatic Change* 43(4): 745–88, December 1999.

JP 99-014. Adjusting to policy expectations in climate change modeling: An interdisciplinary study of flux adjustments in coupled atmosphere-ocean general circulation models, S. Shackley, J. Risbey, P. Stone, and B. Wynne, *Climatic Change* 43(2): 413–54, October 1999. (Also JP Report No. 48)

JP 99-015. Transient climate change and potential croplands of the world in the 21st Century, X. Xiao, C. Vörösmarty, J.M. Melillo, D.W. Kicklighter, H. Tian, A.D. McGuire, Y. Pan, and Z. Yang, *Sistema Terra* 8(1–3):96–109, December 1999.

JP 00-001. Factors affecting heat transport in an ocean general circulation model, I. Kamenkovich, J. Marotzke, and P.H. Stone, *Journal of Physical Oceanography* 30(1): 175–94, January 2000.

JP 00-002. The Kyoto Protocol and developing countries, M. Babiker, J.M. Reilly, and H.D. Jacoby, *Energy Policy* 28: 525–36 (2000). (Also JP Report No. 56)

JP 00-003. Irreversibility, uncertainty, and learning: Portraits of adaptation to long-term climate change, J. Reilly and D. Schimmelpfennig, *Climatic Change* 45: 253–78 (2000).

JP 00-004. A methodology for quantifying uncertainty in climate projections, M.D. Webster and A.P. Sokolov, *Climatic Change* 46(4): 417–46, September 2000. (Also JP Report No. 37)

JP 00-005. Linking local air pollution to global chemistry and climate, M. Mayer, C. Wang, M. Webster, and R.G. Prinn, *J. Geophysical Research* 105(D18): 22,869–96, September 27, 2000. (Also JP Report No. 63)

JP 00-006. Japanese nuclear power and the Kyoto agreement, M. Babiker, J. Reilly, and D. Ellerman, *J. Japanese and International Economies* 14: 169–88. (Also JP Report No. 51)

JP 00-007. A game of Climate Chicken: Can EPA regulate greenhouse gases before the U.S. Senate ratifies the Kyoto Protocol? V. Bugnion and D.M. Reiner, *Environmental Law* 30(3): 491–525 (Summer 2000). (Also JP Report No. 57)

JP 00-008. Supplementarity: An invitation to monopsony? A.D. Ellerman and I. Sue Wing, *Energy Journal* 21(4): 29–59 (October 2000). (Also JP Report No. 59)

JP 00-009. Iron limits the cell division rate of *Prochlorococcus* in the eastern equatorial Pacific, E.L. Mann and S.W. Chisholm, *Limnology and Oceanography* 45(5): 1067–76 (2000).

JP 00-010. Constraining uncertainties in climate models using climate change detection techniques, C.E. Forest, M.R. Allen, P.H. Stone, and A.P. Sokolov, *Geophysical Research Letters* 27(4): 569–72, February 15, 2000. (Also JP Report No. 47)

Massachusetts Institute of Technology
Joint Program on the Science and Policy of Global Change
One Amherst Street (E40-271)
Cambridge, Massachusetts 02139-4307